Investigational New Drugs (2019) 37:935–947
https://doi.org/10.1007/s10637-018-0709-3

PRECLINICAL STUDIES

Screening, identification of prostate cancer urinary biomarkers and verification of important spots

Huijun Zhao[1,2] · Xuhong Zhao[1,2,3] · Ting Lei[1,2,3] · Man Zhang[1,2,3]

Received: 25 October 2018 / Accepted: 5 December 2018 / Published online: 4 January 2019

Summary

Prostate-specific antigen (PSA) has been widely used as the unique serum biomarker for the diagnosis of prostate cancer (PCa). When PSA is moderately increased (e.g., 4–10 ng/ml), it is difficult to differentiate benign prostatic hyperplasia (BPH) from cancer. The diagnostic test (i.e., prostate biopsy) is invasive, adding pain and economic burden to the patient. Urine samples are more convenient, non-invasive and readily available than blood. We sought to determine whether ferritin might be the potential urinary biomarker in prostate cancer diagnosis. Using two-dimensional electrophoresis (2DE) followed by mass spectrometry (MS), differentially expressed urinary proteins among patients with PCa, BPH and normal controls were obtained. The ferritin heavy chain (FTH) gene, ferritin light chain (FTL) gene and protein expression of BPH-1 cells and PC-3 cells were analyzed by real-time quantitative PCR and Western blotting, respectively. Stable FTH or FTL silenced cell lines were generated by small hairpin(sh) RNA lentiviral transfection. The function of the cell lines was evaluated by the colony formation assay, transwell assay, and flow cytometry. Compared with BPH and normal controls, 15 overexpressed proteins, including FTH and FTL, were identified in the urine of the PCa group. FTH and FTL were also highly expressed in PC-3 cell lines compared with BPH-1 cells. FTH-silenced cells showed reduced cell proliferation, migration and increased cell apoptosis. FTL-silenced cells showed increased proliferation and migration abilities. There are differences in urinary proteins among patients with PCa, BPH and normal controls. FTH and FTL play different roles in PCa cells and are potential biomarkers for PCa.

Keywords Urinary proteomics · Prostate cancer (PCa) · Benign prostatic hyperplasia (BPH) · Ferritin · RNA interference

Introduction

In males, PCa is the most common cancer worldwide and the second leading cause of cancer-related death [1]. Since the 1990s, experimental studies focused on prostate cancer have received more attention in our country. Although radical prostatectomy is an effective treatment method, early onset of prostate cancer is difficult to detect, and symptoms of dysuria are similar to those of prostatic hyperplasia. PSA has been widely used as the unique serum biomarker for the diagnosis and/or prediagnosis of PCa. However, this value is the subject of ongoing debates due to the lack of specificity, especially when PSA is moderately increased (e.g., 4–10 ng/ml) [2]. It is generally considered that when the serum PSA measurement is higher than 4 ng/ml, then a prostate biopsy should be performed to confirm the diagnosis. Among men with PSA levels ranging from 4 to 10 ng/ml, 25–40% will have prostate cancer, which means that 60–75% of men with PSA levels ranging from 4 to 10 ng/ml will undergo unnecessary biopsies [3]. As a result, many researchers are working on new potential biomarkers and the molecular pathogenesis of PCa.

In 2004, Rembert et al. [4] eparated nearly 1400 protein spots using two-dimensional electrophoresis (2DE) and identified 150 distinct proteins among 420 spots by mass spectrometry. Using high-resolution LTQ-FT and LTQ-Orbitrap mass spectrometers, Adachi et al. identified 1534 proteins in normal human urine [5].

Ferritin is the major intracellular iron storage protein and is essential for maintaining the cellular redox status. Ferritin is a

✉ Man Zhang
zhangman@bjsjth.cn

[1] Department of Clinical Laboratory, Beijing Shijitan Hospital, Capital Medical University, 10 Tieyi Road, Haidian District, Beijing 100038, China

[2] Beijing Key Laboratory of Urinary Cellular Molecular Diagnostics, Beijing 100038, China

[3] Department of Clinical Laboratory, Peking University Ninth School of Clinical Medicine, Beijing 100038, China

hollow, spherical-structured protein composed of 24 subunits [6]. These 24-mers consist of two gene products: H-ferritin and L-ferritin. Each subunit folds into four helical bundle structures. FTH and FTL share an amino acid sequence homology of 50–56% and are similar in size, but they exhibit distinct functions. The H-ferritin subunit exhibits ferroxidase and antioxidant activity, which converts toxic ferrous ions into less toxic ferric ions. The L-ferritin subunit has no iron oxidase activity, but it can modify the microenvironment to promote the long-term storage of iron and provide an effective site for the formation of iron nuclei, promoting iron nucleation and mineralization. It is also possible that the presence of FTL promotes the turnover rate of FTH ferroxidase activity centers [7]. Clinically, elevated serum ferritin is associated with inflammatory responses such as cancer and autoimmune diseases [8]. In addition, high levels of serum ferritin are also associated with a poor prognosis of the disease [9]. Therefore, not only can ferritin participate in the transport and recycling of iron but also as a biomarker for disease diagnosis and prognosis.

At present, a large number of clinical and epidemiological studies have found that the increase of ferritin in vivo may be related to the development of liver cancer, lung cancer, colon cancer, esophageal cancer, gastrointestinal cancer, pancreatic cancer and breast cancer. When the measured AFP value is low in particular, the ferritin value can be measured as a supplement to improve diagnostic efficiency in liver cancer [10]. Ferritin levels are higher in most tumor tissues than normal tissues. In recent years, ovarian cancer, breast cancer and liver cancer have been the most studied tumors. Previous work in our laboratory has also suggested that ferritin may serve as an important diagnostic indicator of prostate cancer [11]. Here we compared FTH and FTL gene and protein expression in a prostate cancer cell line (PC-3) and a benign prostatic hyperplasia cell line (BPH-1) to confirm their effects. To explore the functions of FTH, FTL in the pathogenesis of prostate cancer, we knocked out the FTH and FTL genes in PC-3 cell lines and observed the effects on the proliferation, apoptosis, migration of prostate cancer cells.

Materials and methods

Materials and study population

Androgen-independent prostate cancer epithelial cells (PC-3) were purchased from the National Infrastructure of the Cell Line Resource (Beijing, China). Human benign prostate hyperplasia epithelial cells (BPH-1) were purchased from the Germany Deutsche Sammlung von Mikroorganismen und Zellkulturen(DSMZ)cell bank. The human FTH, FTL gene shRNA was cloned into the GV248 vector, and its lentivirus was completed by Shanghai GeneChem Co., Ltd. Shanghai, China. The negative control lentiviral vector (5′- TTCTCCGA ACGTGTCACGT -3′) was supplied by Shanghai GeneChem Co., Ltd. Shanghai, China, and it is not homologous to any known human genome. Anti-FTH, FTL human polyclonal antibody, anti-GAPDH human monoclonal antibody and anti-mouse IgG H&L (HRP) were purchased from Abcam Corporation in the United States. TRIzol and SYBR Green fluorescent quantitative PCR kits were purchased from Beijing Dingguo Chang Sheng Company(Beijing,China),. The Annexin V-PE/7-AAD apoptosis detection kit was purchased from BD Company. The PI/RNase dye kit was purchased from Invitrogen Company, transwells from Costar Company, 0.25% trypsin from Genview Corporation, RPMI-1640 from Gibco Company, fetal bovine serum from Beijing Dingguo Chang Sheng Company, and puromycin from the Sigma Company.

The study was approved by the local research ethics boards. The study included 3 patients with PCa, 3 patients with BPH, and 3 age-, gender-, and ethnicity-matched healthy donors who were enrolled at Beijing Shijitan Hospital and Beijing Friendship Hospital. The diagnosis was established by the pathology for all PCa and BPH patients. The control subjects were healthy volunteers with no prior history of cancer and without any chronic urinary tract diseases.

Methods

Urinary protein extraction

The first morning midstream voided urine was collected in a sterile tube from healthy donors and separately from BPH and PCa patients. Fifty milliliters of each sample from a total of 3 patients with cancer were pooled together. The same process applied for the urine of normal volunteers and BPH patients. After centrifugation, the supernatant was used to extract protein using ice-cold acetone. The detailed protocols are described in our previous research[10]. The concentration was calculated by Bradford's methods according to the kit (Sigma-Aldrich, St. Louis, MO, USA). The protein was aliquoted and stored at −80 °C until analysis.

2-DE and Mass spectrometric analysis of urinary proteins

Two-dimensional gel electrophoresis (2-DE) and mass spectrometric analysis were performed as described previously in our laboratory [12]. Briefly, 200 μg protein from each sample in rehydration buffer was loaded for isoelectric focusing (IEF). The maximum volume was 450 μl–500 μl. Solubilized samples were separated using a 24 cm pH 3–10 linear IPG strip for the first dimension. After equilibration, the IPG gel strip was transferred onto 12% SDS-PAGE vertical

gels for the second dimension. The gels were fixed, stained with Coomassie brilliant blue G-250 (Bio-Rad) overnight and destained with deionized water. The PCa, BPH and control samples were assessed simultaneously and repeated 3 times. Every stained 2-DE gel was scanned on an images scanner and analyzed with PDQuest software. Differentially expressed proteins were excised, in-gel digested with trypsin and destained with 100 mmol/L NH_4HCO_3 in 50% acetonitrile. After reduction and alkylation, the proteins were digested with trypsin and 25 mmol/L NH_4HCO_3 at 37 °C overnight. Next, the digested tryptic peptides were extracted with 5% trifluoroacetic acid and 50% acetonitrile with 2.5% trifluoroacetic acid, respectively. Finally, the peptides were subjected to MS analysis. MALDI-TOF/TOF mass spectrometry analysis was performed using an ABI 4700 Proteomics Analyzer. Monoisotopic peptide masses were searched in the IPI human database using MASCOT (Matrix Science) and GPS Explorer (Applied Biosystems).

Cell culture

Androgen-independent prostate cancer epithelial cells (PC-3) and human benign prostate hyperplasia epithelial cells (BPH-1) were cultured in 10% FBS RPMI-1640 medium at 37 °C and 5% CO2. They were digested with 0.25% trypsin for subculturing.

Quantitative real-time PCR (qPCR)

Total RNA was extracted from cells using TRIzol reagent according to the manufacturer's instructions. The extracted RNA samples were reverse-transcribed using a reverse transcription kit. SYBR Green fluorescent quantitative PCR kits were used for qPCR analysis. The reactions were performed in triplicate for each sample in at least three independent runs. Data were analyzed according to the classic $2^{-\Delta\Delta Ct}$ method and normalized to GAPDH expression in each sample. The primers used are listed in Table 1.

Western blot

The total protein in treated cells was extracted using RIPA lysis buffer supplemented with protease inhibitor. The Western blot system was established using a Bis-Tris Gel system and polyvinylidene fluoride (PVDF) membranes according to the manufacturer's instruction. Primary antibodies were prepared in 5% blocking buffer at a dilution of 1:1000 and incubated with the membranes at 4°C overnight, followed by washing and incubation with secondary antibodies conjugated to horseradish peroxidase for 2 h. The densitometry of the protein bands was quantified and the values expressed relative to β-actin. All experiments were repeated three times.

Generation of stable cell lines

Cells were seeded into 96-well plates at 1×10^3 per well and incubated for 24 h at 37 °C. After growth to 50% confluence, either FTH, FTL shRNA construct or control vector were transfected into PC-3 cells according to the manufacturer's protocols, followed by selection with 2 μg/ml puromycin for 2 weeks. Antibiotic-resistant clones were isolated in medium with 1 μg/ml puromycin. The cells were divided into the control group (PC-3), negative control group (NC group, with nonspecific small interfering (shRNA-NC), LV-shFTH-1 group, LV-shFTH-2 group and LV-shFTH-3 group (with the FTH gene silenced by RNA interference (RNAi 1, RNAi 2, RNAi 3), LV-shFTL-1 group, LV-shFTL-2 group and LV-shFTL-3 group (with the FTL gene silenced by RNA interference (RNAi 4, RNAi 5, RNAi 6). All siRNA sequences were synthesized by Shanghai GeneChem Co., Ltd. Shanghai, China. Sequences of shFTH-1, shFTH-2, shFTH-3, shFTL-1, shFTL-2, and shFTL-3 are shown in Table 2. RT-PCR and Western blotting were performed to confirm the knockdown of mRNA and protein of FTH, FTL in the transfectants.

Colony formation assay

LV-shFTH, shFTL and NC group cells were trypsinized, resuspended and inoculated into 6-well plates at densities of 200 cells per well. The medium was replaced every week. Cells plated in the 6-well plates were incubated for 14 days, and the formed colonies were fixed with paraformaldehyde and stained with crystal violet for 20 min, respectively. After washing the cells with double-distilled water, the clusters were imaged, and the number of colonies were counted.

Transwell assay

The transwell assay was performed using transwell chambers, in which 1×10^4 NC cells, LV-shFTH cells or LV-shFTL cells were seeded in the upper chamber of a 24-well plate with 200 μl medium containing 3% FBS. The lower chamber was filled with 500 μl medium containing 10% FBS to induce cell migration. The chamber was incubated at 37 °C for 24 h. At the end of incubation, the cells on the upper surface of the membrane were removed with a cotton swab. The cells that had migrated to the lower surface of the membrane were stained with crystal violet. Images were obtained using a CKX41 inverted microscope (Olympus), and the cells were counted in ten different fields of view using NIH ImageJ software. The experiment was conducted in triplicate.

Flow cytometry

For the detection of apoptosis, infected cells were collected, washed two times with ice-cold PBS, and resuspended at

Table 1 The primers used in real-time quantitative PCR (qRT-PCR)

Gene	Forward primer	Reverse primer
FTH	5′- CATCAACCGCCAGATCAAC -3’	5′- GATGGCTTTCACCTGCTCAT −3’
FTL	5′- CAGCCTGGTCAATTTGTACCT −3’	5′- GCCAATTCGCGGAAGAAGTG −3’
GAPDH	5′- TTTGGTATCGTGGAAGGACT −3’	5′- AGTAGAGGCAGGGATGATGT −3’

1*10^6 cells/ml in 1 × binding buffer. To 100 μl of the cell suspension was added 5 μl Annexin V-PE and 5 μl 7-AAD, followed by incubation at room temperature for 15 min and addition of 400 μl 1X binding buffer to each tube. Flow cytometry was used to detect the cells after 1 h.

For cell cycle detection, the collected cells were washed two times with precooled PBS, followed by the addition of precooled 70% alcohol and an overnight incubation at 4 °C overnight. The collected cells were washed two times with precooled PBS, followed by the addition of 0.5 ml PI/RNase dye. The cells were incubated in the dark for 30 min. Flow cytometry was used to detect the cells after 1 h.

Statistical analysis

All data collected from independent experiments are expressed as the mean ± standard deviation (SD). Statistical analyses were performed using GraphPad Prism 6.0 statistical software (GraphPad Software Inc., La Jolla, USA). The Student’s t test was used to evaluate differences between the LV-NC cells and LV-shFTH cells or LV-shFTL cells using SPSS 17.0 software (IBM Corp., Armonk, NY, USA). Multiple groups were compared using one-way ANOVA (one-way ANOVA). A $P < 0.05$ was considered to indicate a statistically significant result.

Results

Urinary proteomic profiles of normal controls, BPH and PCa

To increase the quantity of different proteins in urine, urinary proteins were extracted from pools of three patients’ urine for each group. The specific information for the patients and statistical analysis of FCR are presented in Table 3. A pH 3–10 nonlinear IPG strip was used to separate the extracted proteins, followed by 2-DE and CBB staining. We established the urinary proteomic profiles of normal controls, BPH and PCa (Fig. 1A-C). More than 1000 spots were detected on the 2-D gel with a molecular weight range from 10 to 100 KDa. Thirty upregulated protein spots in PCa compared with BPH and controls were identified by MALDI-TOF mass spectrometry. The positions of the 30 spots were marked on the 2-D gel profile of PCa (Fig. 1D).

Identification of 30 overexpressed protein spots in the PCa groups by MALDI-TOF-MS

To identify individual proteins, the 30 upregulated protein spots were cut out and subjected to in-gel trypsin digestion. The PMF maps obtained by MALDI-TOF MS were used for protein identification. Fifteen different kinds of proteins were matched, including cytoskeletal protein and related proteins (spot 5, 24, 30), plasma factor (spot 25), enzyme (spot 28), and lipocalin proteins (spot 12, 16, 27, 29), membrane proteins (spot 11, 13), transcriptional correlation factor (spot 8), and unknown proteins (spot 4, 17, 26). The detailed information from the database is shown in Table 3.

GO enrichment analysis of differentially expressed genes

All differential proteins were mapped to each term of the gene ontology database, the number of proteins for each term was calculated, and then a hypergeometric test was used to identify the GO items that were significantly enriched in the differential proteins. The GO enrichment analysis is illustrated in Fig. 2. For example, Fig. 2A shows the biological process in which the differential genes participate, Fig. 2B shows the molecular function of the differential genes, and Fig. 2C shows the location of the differential genes. The items shown in the figure indicate a significance level less than 0.05 by Fisher’s exact test in each category. GO enrichment analysis showed that the biological processes of the differential proteins included intracellular sequestration of iron ion and iron ion transport, among others (Fig. 2A); the molecular functions were mainly involved in protein binding and identical protein binding (Fig. 2B); and the cellular component of the

Table 2 The sequences of NC, three shRNA against FTH and three shRNA against FTL

Gene	Target sequence (5′-3′)
shFTH-1	TGTCCATGTCTTACTACTT
shFTH-2	GGCGGAATATCTCTTTGACAA
shFTH-3	GAGAGGGAACATGCTGAGAAA
shFTL-1	GCCACTTCTTCCGCGAATTGG
shFTL-2	GCGCTCTCTTCCAGGACATCA
shFTL-3	GGAGACTCACTTCCTAGATGA
NC	TTCTCCGAACGTGTCACGT

Table 3 30 over-expressed protein spots in PCa groups identified by MALDI-TOF-MS

Spot No.	Swiss-Prot	Protein name	Mass(Da)	PI	function
1, 2, 7,20	P02760	AMBP Protein	38,974	5.95	Protease inhibitor
3,18,21	B4DPR2	cDNA FLJ50830, highly similar to AMBP	29,759.4	6.01	transport
4	–	unnamed protein product	13,595.7	4.79	–
5	Q08AD1	Isoform 2 of Calmodulin-regulated spectrin-associated protein 1-like 1 (CAMSAP1L1)	164,895	6.23	Protein binding
6,22,23	B7Z8R6	cDNA FLJ51445, highlysimilar to AMBP protein	29,759.4	6.01	Binding; transporter activity
8	O00164	Ribosomal RNA upstream binding transcription factor (Fragment, UBTF)	75,892.2	8.78	DNA binding
11,13	P98160	Basementmembrane-specific heparan sulfate proteoglycan coreprotein (HSPG2)	468,500	6.06	Lipoprotein lipase activity; protein C-terminus binding
12	P02794	Ferritin heavy chain (FTH1)	21,212.3	5.3	Ferric iron binding; ferroxidase activity; protein binding
16,27	P02766	Transthyretin; 13 kDa protein	13,146.4	5.34	Hormone activity
17	–	Unknown (protein for IMAGE:3934797)	22,637.5	8	Unknown (protein for IMAGE:3934797)
24	Q9BYX7	Putative beta-actin-like protein 3	41,988.8	5.91	ATP-binding
25	P08709	F7 Factor VII active sitemutant immunoconjugate	75,504.4	6.6	Calcium ion binding; glycoprotein binding; serine-type endopeptidase activity
26	Q9H0W9	C11orf54	33,076.7	6.64	hydrolase
28	Q03154	Aminoacylase-1 (ACY1)	55,958.8	6.56	Aminoacylase actibity; metal ion binding; metallopeptidase activity
29	P02792	Ferritin Light chain (FTL)	21,282.8	5.7	Ferric iron binding; identical protein binding; oxidoreductase activity
30	Q14019	Coactosin-like protein (COTL1)	15,935	5.54	Actin binding; enzyme binding

differential proteins was mainly extracellular exosome (Fig. 2C). A combination of the data presented in Fig. 2A and B is shown in Fig. 2D, which included all proteins based on both molecular function and biological process. However, these targets were all predictions and were not validated by the experiment.

FTH and FTL were included among the 15 upregulated proteins

Spot 12 was overexpressed in PCa and subsequently identified as FTH1 by MALDI-TOF (Fig. 3A). Spot 29 was overexpressed in PCa and subsequently identified as FTL by MALDI-TOF-MS (Fig. 3B). Among 15 different kinds of proteins, we chose for further study the upregulated protein ferritin, which consisted of ferritin heavy chain and ferritin light chain. We attempted to determine whether FTH and FTL might be potential urinary biomarkers in prostate cancer diagnosis.

FTH and FTL were overexpressed in PC-3 cell lines compared with BPH-1

To detect the expression levels of FTH, FTL in prostate cancer cells (PC-3) and benign prostate hyperplasia epithelial cells (BPH-1), we used a Lane 1D gel analysis system to analyze the gray value of the bands (Fig. 4). β-actin served as the reference. We performed a semiquantitative analysis on each set of data. The experiments were repeated three times. The protein expression of FTH (Fig. 4A), FTL (Fig. 4B) was higher in PC-3 cells than BPH-1 cells.

Generation of stable shFTH cell lines; downregulation of FTH inhibited colony formation, migration ability of PC-3 cell, facilitated PC-3 cell's apoptosis and induced cell cycle arrest in G1 phase

At 72 h after the lentiviruses were transfected into PC-3 cells, Western blotting was used to detect the FTH protein level, which revealed that compared with the control and shRNA/Control (NC) groups, the protein levels of FTH in the shFTH-1, shFTH-2 and shFTH-3 groups were markedly decreased (all $P < 0.05$), but there was no significant difference in the protein level between the control and NC groups ($P > 0.05$) (Fig. 5A). Therefore, the shFTH-1 group (named as shFTH group) was chosen for further experiments. After the lentivirus was transfected with PC-3 cells and two month of puromycin selection, we detected the efficiency of lentivirus infection under a fluorescence microscope. The results showed that

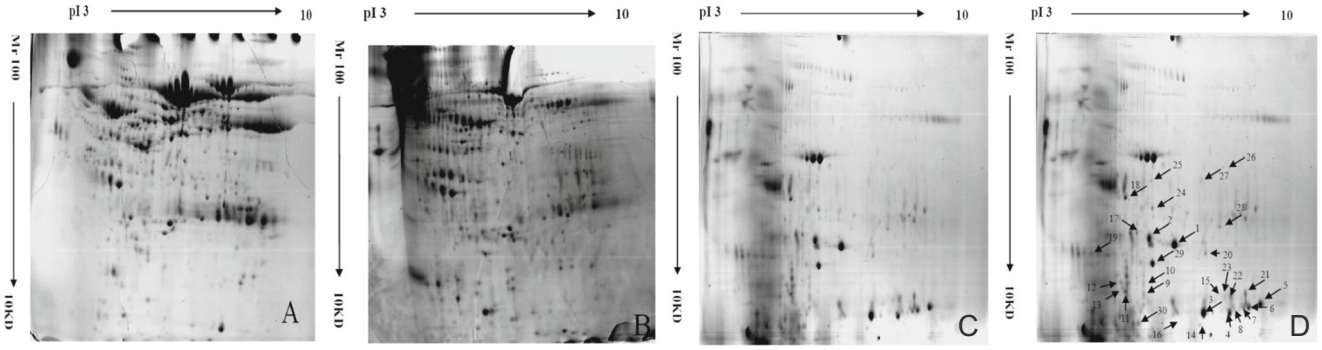

Fig. 1 Urinary proteomic profiles of normal controls, BPH and PCa. Concentrated urine protein (200 μg) derived from normal controls (A), BPH (B), or patients with PCa (C) was separated by 2-DE, which included a first dimension of IPG (pH 3 to 10) and a second dimension of 12% SDS-PAGE. More than 1000 spots were detected on the 2-D gel with a molecular weight range from 10 to 100 KDa and pH range from 3 to 10. Thirty differentially expressed protein spots were excised individually from the gel for prostate cancer (D). The detected protein spots were marked, numbered and excised for further analysis

the cell infection efficiency was greater than 90% in the two groups, as shown in Fig. 5A. The mRNA expression levels in the LV-shFTH cells were markedly decreased, as shown in Fig. 5A.

The colony formation assay results confirmed that the colony formation ability of cells in each group was distinctly different. Compared with the NC group (0.24 ± 0.01), the colony formation ability of cells in the LV-shFTH group (0.05 ± 0.01) was significantly reduced (Fig. 5B, $P < 0.05$). A transwell assay was employed to examine the role of FTH in cellular migration. As shown by the transwell assay results presented in Fig. 5C, the number of cells after 24 h in 10 fields under the microscope at 400x was 33 ± 3 in the negative control group and 3 ± 1.5 in the LV-shFTH group. The difference was statistically significant. The cell migration ability significantly declined in the LV-shFTH group compared with the NC group. Flow cytometry showed that the apoptosis index was 4.37 ± 0.42 in the NC

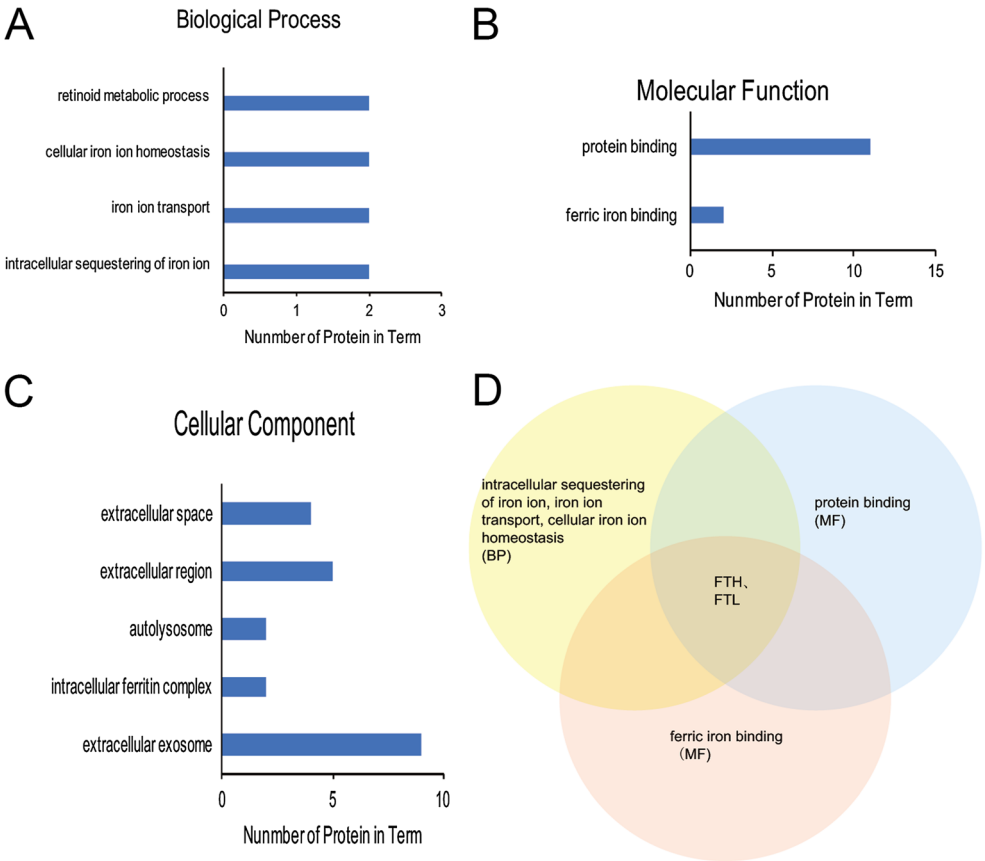

Fig. 2 Classification of differentially expressed proteins based upon their annotations in the database. Distribution of differentially expressed proteins in terms of (A) biological processes, (B) molecular functions and (C) cellular components. (D) Transformation of (A) and (B) to a pie diagram to directly show the intersection of proteins on aspects of both MF and BP

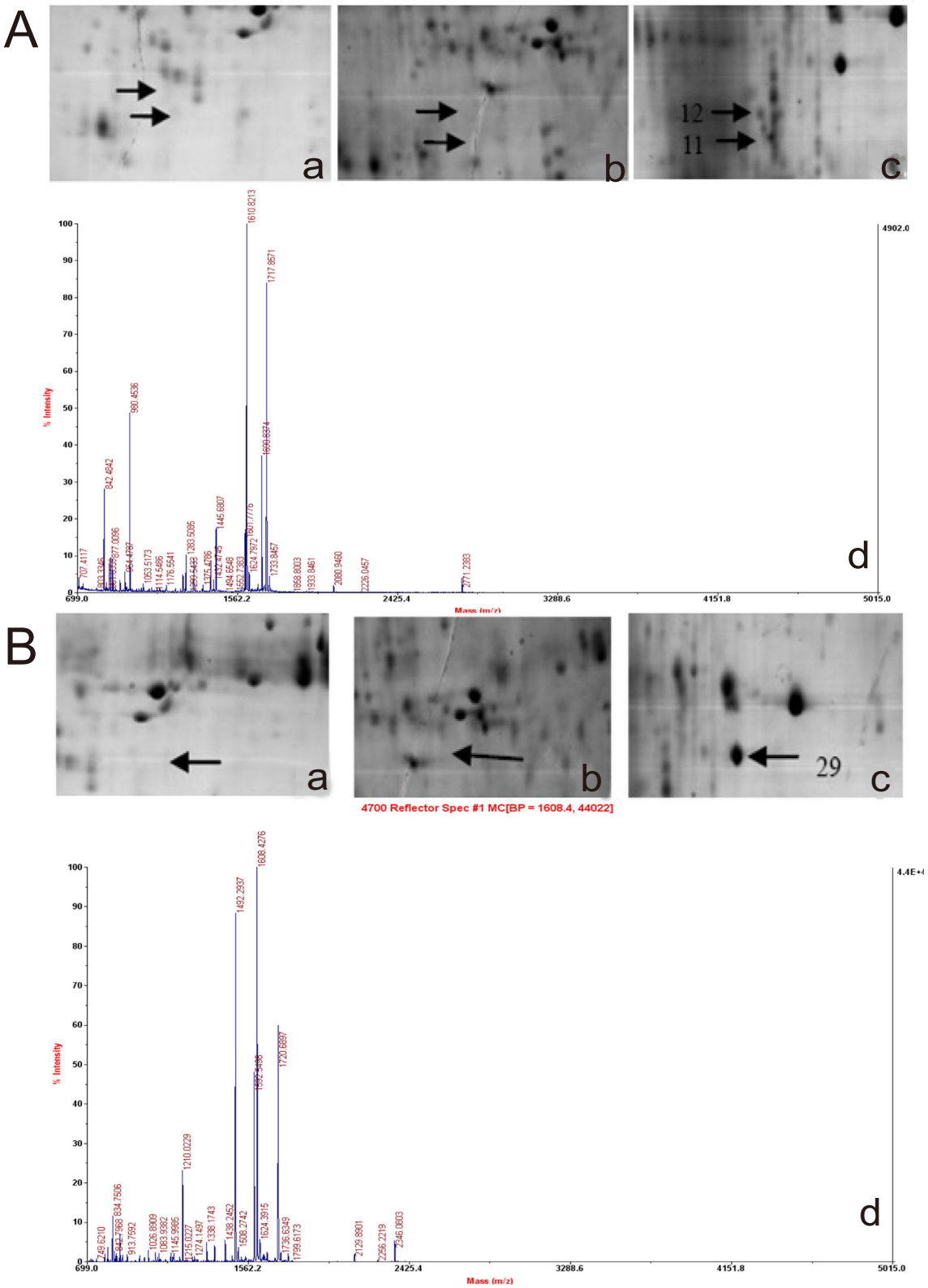

Fig. 3 Differential expression of spot 12 and 29 among the three groups and its PMF map. Upper maps showed the position and expression of spot 12 (A) and 29 (B) in the normal control (a), BPH (b) and PCa group (c), respectively

group and 8.5 ± 0.6 in the LV-shFTH group ($P < 0.05$). The apoptosis rate was higher in the FTH interference group than the negative control group (Fig. 5D). The ratio of PC-3 cells in G1 phase was higher in the LV-shFTH group than

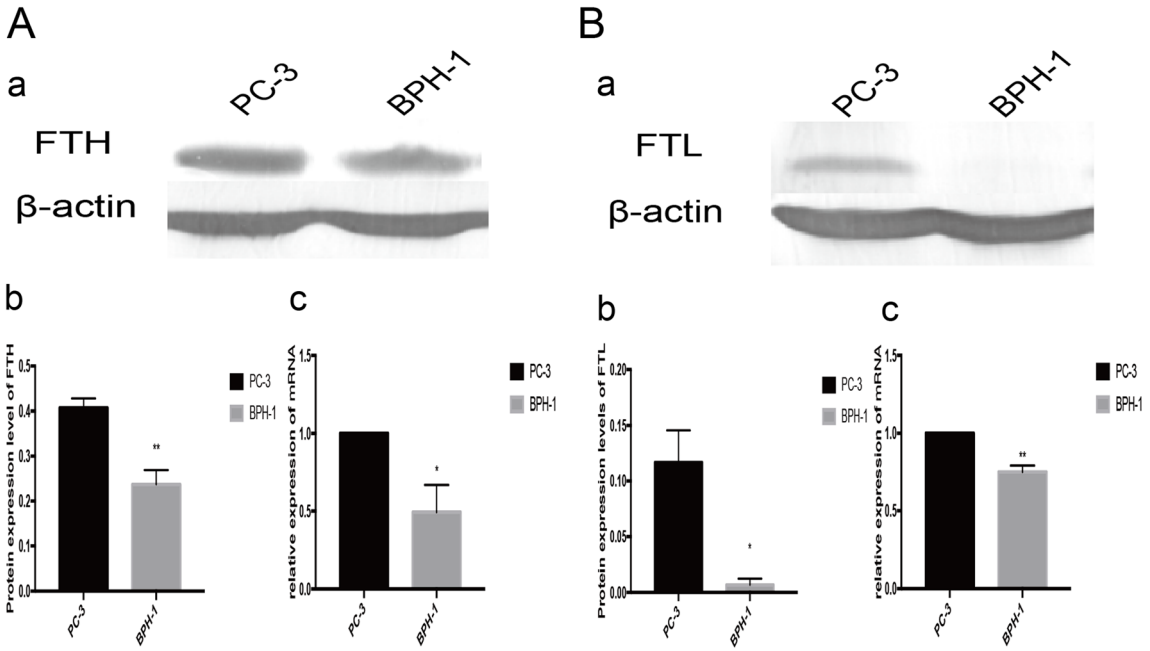

Fig. 4 Differential expression of FTH, FTL in PC-3 cells and BPH-1 cells. (A) A representative image of the Western blot and qPCR graph of PC-3 cells with higher FTH expression, compared to BPH-1. (B) A representative image of the Western blot and qPCR graph of PC-3 cells with higher expression of FTL, compared to BPH-1. (a, b) A representative image of the Western blot. (d) A representative qPCR graph. * $P < 0.05$; ** $P < 0.01$

in the NC groups. The ratio of cells in S and G2 phase was lower in the LV-shFTH group than the NC groups (Fig. 5E, $P < 0.05$). These results showed that FTH gene silencing could arrest PC-3 cells in G1 phase.

Generation of stable shFTL cell lines; downregulation of FTL enhanced the colony formation and migration abilities of PC-3 cell

Additionally, the protein levels of FTL in the shFTL-1, shFTL-2 and shFTL-3 groups were markedly decreased (all $P < 0.05$), but there was no significant difference in protein levels between the control and NC groups ($P > 0.05$) (Fig. 6A). Therefore, the shFTL-1 group (named as shFTL group) was chosen for further experiments. After the PC-3 cells were transfected with lentivirus and two months of puromycin selection, the efficiency of cell infection was found to be greater than 90% in the two groups, as shown in Fig. 6A. The mRNA expression levels in the LV-shFTL cells were markedly decreased, as shown in Fig. 6A. FTL was obviously inhibited after 72 h and could be inhibited over the long term.

The colony formation assay validated that compared with the NC group (0.24 ± 0.01), the colony formation ability of cells in the LV-shFTL group (0.60 ± 0.03) was significantly increased (Fig. 6B, $P < 0.01$). A transwell assay was also employed to examine the role of FTL in cellular migration. As shown by the transwell assay results presented in Fig. 6C, the number of cells after 24 h in 10 fields under the microscope at 400x was 33 ± 3 in the negative control group and 285 ± 13.2 in the LV-shFTL group. This difference was statistically significant. Cell migration ability was significantly increased in the LV-shFTL group compared with the NC group. Flow cytometry showed that the apoptosis index was 4.37 ± 0.42 in the NC group and 8.5 ± 0.6 in the LV-shFTL group ($P > 0.05$). The apoptosis rates were not significantly different between the FTL interference and negative control groups (Fig. 6D). The ratio of PC-3 cells in G2 phase was lower in the LV-shFTL group than the NC groups (Fig. 6E, $P < 0.05$).

Discussion

Prostate cancer-related morbidity and mortality are on the rise In Asia [13]. The current diagnosis of prostate cancer relies mainly on measuring the level of total serum prostate-specific antigen (PSA), which may lead to overdiagnosis or

Fig. 5 Infection of PC-3 cells by LV-shFTH lentivirus: comparison of cell colony formation abilities, cell migration, cell cycle and apoptosis between the NC and LV-shFTH groups. Notes A: (a) Representative images of the lentivirus infection efficiency of PC-3. After puromycin selection, the lentivirus infection efficiency reached nearly 100% (X100). FTH was obviously inhibited after 72 h and would be inhibited over the long term. (b) The gray value for the β-actin and FTH protein bands; (c) protein levels of FTH; (d) mRNA expression levels of FTH; B: colony morphology and efficiency of colony formation; C: representative images and transwell migration assay graphs of NC cells and LV-shFTH cells; D: cell apoptosis by FCM and apoptosis rates of cells; and E: number and ratios of cells in S, G1and G2 phase (all experiments were repeated three times, *P < 0.05, **P < 0.01) ▶

overtreatment of prostate cancer [14]. Most of the spots identified in our results were plasma secreted proteins and proteolytic degradation. Among them, spots 12 and 29 were ferritin heavy chain and light chain, respectively. Based on Table 3, we concluded that most proteins in urine consisted of a variety of albumin degradation products (spots 1, 2, 3, 6, 7, 18, 20, 21, 22, 23). These results were consistent with a former study. Spots 11 and 13 were proteolytic degradation products of

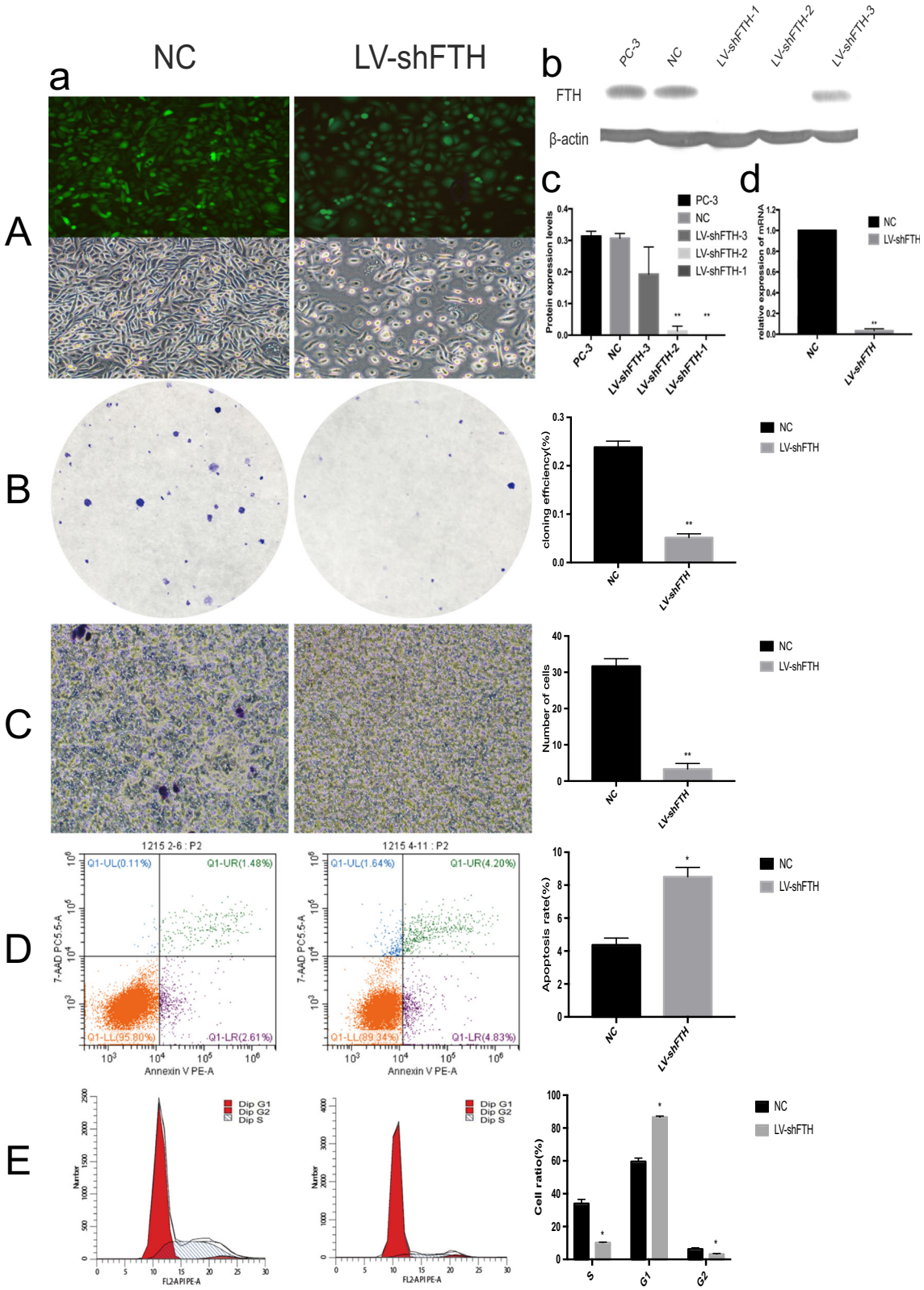

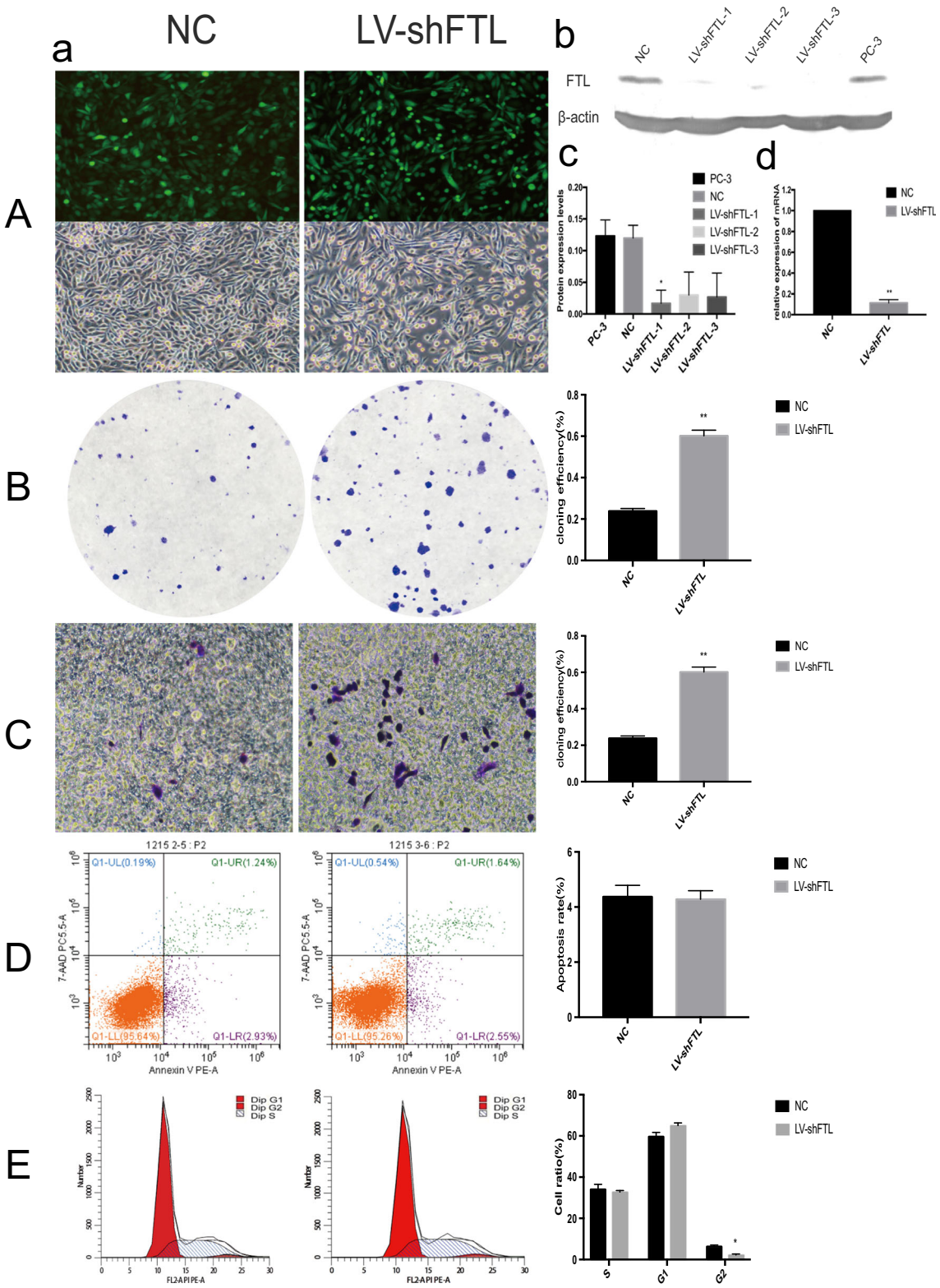

extracellular matrix. Spots 12, 16, 27 and 29 were plasma proteins. Spots 5, 8, 24 and 30 were identified as cell apoptosis proteins. Wang et al. have demonstrated that serum ferritin combined with PSA enhances the predictive accuracy of prostate cancer [15]. In addition, our laboratory's preliminary study demonstrated representative immunohistochemical expression of FTL and FTH, with strong staining intensities in the prostate cancer group (PCa) and weak staining intensity in the benign prostatic hyperplasia group (BPH). Furthermore, differences in the urinary ferritin-creatinine ratio (FCR) were

◀ **Fig. 6** Infection of PC-3 cells by LV-shFTL lentivirus: comparison of cell colony formation abilities, cell migration, cell cycle and apoptosis between the NC and LV-shFTL groups. Notes A: (a) Representative images of the lentivirus infection efficiency of PC-3. After puromycin selection, the lentivirus infection efficiency reached nearly 100% (X100). FTL was inhibited after 72 h and could be inhibited over the long term. (b) The gray value for the β-actin and FTL protein bands; (c) protein levels of FTL; (d) mRNA expression levels of FTL; B: colony morphology and efficiency of colony formation; C: representative images and transwell migration assay graphs of NC cells and LV-shFTL cells; D: cell apoptosis by FCM and apoptosis rates of cells; and E: number and ratios of cells in S, G1and G2 phase (all experiments were repeated three times, *P < 0.05, **P < 0.01)

observed among the three groups, with significant differences in the PCa group compared with both the BPH and control groups. In contrast, there were no significant differences between the BPH and N groups [11]. This finding suggests that ferritin may serve as an important diagnostic indicator of prostate cancer. To further confirm the effect of FTL and FTH on the biological behavior of prostate cancer cells, we knocked down the expression of FTL and FTH in the prostate cancer cell line PC-3 by lentivirus-mediated RNA interference and observed the effect on prostate cancer cell proliferation, apoptosis, migration ability and tumorigenicity, with the goal of providing preliminary experimental data to explore the functional role of FTL and FTH in the pathogenesis of prostate cancer and their potential as clinical treatment targets for prostate cancer.

The results showed that FTH and FTL were overexpressed in the PC-3 cell lines compared with BPH-1. In particular, knockdown of FTH reduced cell proliferation, migration and contributed to cell apoptosis. In contrast, knockdown of FTL contributed to cell proliferation and migration. The iron absorption process requires the cooperation of the H and L subunits. Ferritin is localized in the cytoplasm, mitochondria and nucleus in eukaryotes. Cytoplasmic ferritin consists of 24 heavy chains (H; FHC; FTH) and light chain (L; FTL) ferritin subunits that can hold up to 4500 iron atoms in the central compartment [16]. In humans, the molecular weights are 21 and 19 kDa, respectively [17, 18]. Two different genes encoding heavy and light subunits belong to a complex polygenic family and are regulated by different transcriptional mechanisms, while the mitochondrial forms are encoded by no intronic H-type genes [19, 20]. Despite its broad homology, FTH and FTL have different functions: FTH has iron oxidase activity that favors the rapid uptake and release of iron, while FTL contributes to the long-term storage of iron [20].

Ferritin is differentially overexpressed in the tissues of a variety of malignancies including hepatocellular carcinoma [21],Hodgkin lymphoma [22],breast cancer [23],pancreatic cancer [24] and prostate cancer [11]. Structural and immunological analyses have revealed that the composition of the tumor ferritin subunit is different, most likely caused by different proportions of the L and H subunits [25]. The composition of the ferritin complex varies in different tissues based on their iron requirements and metabolism patterns. For example, H-ferritin is abundant in heart, muscle, brain, and kidney, while L-ferritin is rich in liver and spleen, and this ratio is very easily altered during a state of inflammation, foreign stimulation and differentiation [26]. The human protein map data shows that the ferritin light chain (http://www.proteinatlas.org/ENSG00000087086/normal) is highly expressed in the CNS, spleen, bone marrow, liver, lung, kidney, and adipocytes. The expression of the heavy chain (http://www.proteinatlas.org/ENSG00000167996/normal) is roughly the same, and it is also highly expressed in the prostate, breast, testis, uterus and thyroid tissues. However, the actual stoichiometries of the subunit ratios of ferritin in different tissues are unknown, thus also influencing the ranking or crystallinity of the mineral core [27]. Therefore, the present findings for ferritin light and heavy chains might reveal opposite results. However, further evidence is needed to validate these findings.

In breast cancer cells, Yang, et al. have shown that the downregulation of ferritin in MCF-7 cells results in cell growth inhibition through increased apoptosis, mediated by decreased levels of Bcl-2 mRNA [28]. Lobello et al. have demonstrated that low FTH expression is associated with a poor prognosis in ovarian cancer and that sFOV3 cells have a stronger tumorigenic phenotype after FTH silencing [29]. There is growing evidence that ferritin is involved not only in intracellular iron metabolism but also many biochemical pathways involved in the development and progression of cancer. Min Pang and Connor et al. demonstrated that these pathways include control of cell proliferation, inhibition of cell death and apoptosis, and induction of epithelial-mesenchymal transition [30]. The specific role of ferritin in these intricate processes has not yet been completely determined. Conflicting results may also derive from specific differences in the cells.

In addition to its role in iron metabolism, ferritin is also involved in many cellular regulatory pathways, such as proliferation [26], chemokine signaling [31] and angiogenesis [32]. In HeLa cells, Cozzi et al. found that high expression of H- but not L-ferritin resulted in a reduction of apoptosis by approximately 50%. This anti-apoptotic activity is independent of ferroxidase activity as overexpression of mutant ferritin with an inactive ferroxidase center shows a similar effect [33]. In addition, H-ferritin has also been found to be an important mediator of the anti-apoptotic activity of NFkB during the inflammatory response. This activity is achieved by iron chelation and ROS inhibition and subsequent inhibition of pro-apoptotic c-JNK signaling [21]. In human malignant mesothelioma cells, constitutively expressed H-ferritin has been shown to protect H_2O_2-induced apoptosis, whereas downregulation of H-ferritin results in increased sensitivity [34]. Coffman et al. reported that high-molecular-weight kininogen (HKa) is inactivated after binding to ferritin, whereas HKa is

an angiogenic inhibitor [35]. It was further demonstrated that both H- and L-ferritin can block the anti-angiogenic effect of HKa [36]. H-ferritin, but not L-ferritin or H-ferritin mutants lacking iron oxidase, can bind to DNA [37]. Thompson et al. have also found that H-ferritin preferentially translocates to the nucleus, protecting DNA from iron-induced oxidative damage [38]. These studies results are consistent with the findings of our experiments.

Although elevated serum ferritin is observed in quite a few cancers, the source of the elevated serum ferritin has not been directly addressed. As an example, although liver cancer cells can secrete ferritin in vitro [39], some recent in vivo studies have suggested that serum ferritin is predominantly derived from macrophages rather than hepatocytes [40]. Similarly, studies have demonstrated that a higher level of ferritin is detected in both serum and tumor lysates of breast cancer patients, and its increase is associated with a poor prognosis. Ferritin stimulates breast cancer cells through an iron-dependent mechanism and is localized to tumor-associated macrophages [23]. The effector and molecular mechanism by which tumor-associated macrophages affect tumorigenesis remain unclear. Thus, while high ferritin levels are positively correlated with increased serum PSA levels and prostate cancer risk [15], serum ferritin levels may also produce conflicting results in vitro.

We will continue to explore the expression of FTH and FTL in prostate cancer tissue samples and its clinical significance, as well as screen and identify important interaction effector molecules and signaling pathways involved in the regulation of FTH, FTL. Determination of the mechanism of action of FTH, FTL in prostate progression will help to further improve the pathogenesis of prostate cancer and provide a new biomarker and an important theoretical basis for the diagnosis of prostate cancer.

In conclusion, we separated more than 1000 spots on a 2-DE gel using urine samples. Among these spots, 15 different kinds of upregulated proteins were identified, including FTL and FTH1, consistent with previous research. FTH and FTL play significant roles in the proliferation, apoptosis and migration of prostate cancer cells, suggesting that they may be crucial candidate cancer relevant genes involved in the formation and progression of prostate cancer. These analyses will help to further distinguish PCa patients from BPH patients, clarify the pathogenesis of prostate cancer and provide an important basis for the diagnosis of prostate cancer in clinical work.

Compliance with ethical standards

Conflicts of interest Huijun Zhao, Xuhong Zhao, Ting Lei, Man Zhang declare that they have no conflicts of interest.

Funding This work was supported by the Beijing Municipal Administration of Hospitals' Ascent Plan (DFL20150701) and the Beijing Natural Science Foundation (7172106).

Ethical approval All procedures performed in studies involving human participants were conducted in accordance with the ethical standards of the institutional and/or national research committee and with the 1964 Helsinki declaration and its later amendments or comparable ethical standards. This article does not contain any studies with animals performed by any of the authors.

Informed consent Informed consent was obtained from all individual participants included in the study.

References

1. Siegel RL, Miller KD, Jemal A (2018) Cancer statistics, 2018. CA Cancer J Clin 68(1):7–30. https://doi.org/10.3322/caac.21442
2. Thompson IM (2004) Prevalence of prostate cancer among men with a prostate-specific antigen level <= 4.0 ng per milliliter (vol 350, pg 2239, 2004). N Engl J Med 351(14):1470–1470
3. Andriole GL, Levin DL, Crawford ED, Gelmann EP, Pinsky PF, Chia D, Kramer BS, Reding D, Church TR, Grubb RL, Izmirlian G, Ragard LR, Clapp JD, Prorok PC, Gohagan JK, Team PP (2005) Prostate Cancer screening in the prostate, lung, colorectal and ovarian (PLCO) Cancer screening trial: findings from the initial screening round of a randomized trial. J Natl Cancer Inst 97(6):433–438. https://doi.org/10.1093/jnci/dji065
4. Pieper R, Gatlin CL, McGrath AM, Makusky AJ, Mondal M, Seonarain M, Field E, Schatz CR, Estock MA, Ahmed N, Anderson NG, Steiner S (2004) Characterization of the human urinary proteome: a method for high-resolution display of urinary proteins on two-dimensional electrophoresis gels with a yield of nearly 1400 distinct protein spots. Proteomics 4(4):1159–1174
5. Adachi J, Kumar C, Zhang YL, Olsen JV, Mann M (2006) The human urinary proteome contains more than 1500 proteins, including a large proportion of membrane proteins. Genome Biol 7(9)
6. Crichton RR, Declercq JP (2010) X-ray structures of ferritins and related proteins. Biochim Biophys Acta 1800(8):706–718. https://doi.org/10.1016/j.bbagen.2010.03.019
7. Knovich MA, Storey JA, Coffman LG, Torti SV, Torti FM (2009) Ferritin for the clinician. Blood Rev 23(3):95–104. https://doi.org/10.1016/j.blre.2008.08.001
8. VanWagner LB, Green RM (2014) Elevated serum ferritin. JAMA 312(7):743–744. https://doi.org/10.1001/jama.2014.302
9. Alkhateeb AA, Connor JR (2013) The significance of ferritin in cancer: anti-oxidation, inflammation and tumorigenesis. Biochim Biophys Acta 1836(2):245–254. https://doi.org/10.1016/j.bbcan.2013.07.002
10. Cujic D, Golubovic S, Bojic-Trbojevic Z, Ilic N, Baricevic I, Nedic O (2010) Differential diagnosis of liver diseases using serum biomarkers. J BUON 15(1):141–146
11. Su Q, Lei T, Zhang M (2017) Association of ferritin with prostate cancer. J BUON 22(3):766–770
12. Meng Q, Lei T, Zhang M, Zhao J, Zhao XH, Zhang M (2013) Identification of proteins differentially expressed in adriamycin-resistant (pumc-91/ADM) and parental (pumc-91) human bladder cancer cell lines by proteome analysis. J Cancer Res Clin Oncol 139(3):509–519. https://doi.org/10.1007/s00432-012-1350-8
13. Ito K (2014) Prostate cancer in Asian men. Nat Rev Urol 11(4):197–212. https://doi.org/10.1038/nrurol.2014.42
14. Tabayoyong W, Abouassaly R (2015) Prostate Cancer screening and the associated controversy. Surg Clin N Am 95(5):1023. https://doi.org/10.1016/j.suc.2015.05.001
15. Wang XJ, An P, Zeng JL, Liu XY, Wang B, Fang XX, Wang FD, Ren GP, Min JX (2017) Serum ferritin in combination with

prostate-specific antigen improves predictive accuracy for prostate cancer. Oncotarget 8(11):17862–17872
16. Arosio P, Levi S (2010) Cytosolic and mitochondrial ferritins in the regulation of cellular iron homeostasis and oxidative damage. Biochim Biophys Acta Gen Subj 1800(8):783–792. https://doi.org/10.1016/j.bbagen.2010.02.005
17. Boyd D, Vecoli C, Belcher DM, Jain SK, Drysdale JW (1985) Structural and functional relationships of human ferritin H and L chains deduced from cDNA clones. J Biol Chem 260(21):11755–11761
18. Arosio P, Adelman TG, Drysdale JW (1978) On ferritin heterogeneity. Further evidence for heteropolymers. J Biol Chem 253(12):4451–4458
19. Alkhateeb AA, Connor JR (2010) Nuclear ferritin: a new role for ferritin in cell biology. Biochim Biophys Acta Gen Subj 1800(8):793–797. https://doi.org/10.1016/j.bbagen.2010.03.017
20. Arosio P, Ingrassia R, Cavadini P (2009) Ferritins: a family of molecules for iron storage, antioxidation and more. Biochim Biophys Acta Gen Subj 1790(7):589–599. https://doi.org/10.1016/j.bbagen.2008.09.004
21. Kew MC, Torrance JD, Derman D, Simon M, Macnab GM, Charlton RW, Bothwell TH (1978) Serum and tumour ferritins in primary liver cancer. Gut 19(4):294–299
22. Eshhar Z, Order SE, Katz DH (1974) Ferritin, a Hodgkin's disease associated antigen. Proc Natl Acad Sci U S A 71(10):3956–3960
23. Alkhateeb AA, Han B, Connor JR (2013) Ferritin stimulates breast cancer cells through an iron-independent mechanism and is localized within tumor-associated macrophages. Breast Cancer Res Treat 137(3):733–744
24. Marcus DM, Zinberg N (1974) Isolation of ferritin from human mammary and pancreatic carcinomas by means of antibody immunoadsorbents. Arch Biochem Biophys 162(2):493–501
25. Arosio P, Yokota M, Drysdale JW (1976) Structural and immunological relationships of isoferritins in normal and malignant cells. Cancer Res 36(5):1735–1739
26. Torti FM, Torti SV (2002) Regulation of ferritin genes and protein. Blood 99(10):3505–3516
27. Theil EC (2011) Ferritin protein Nanocages use ion channels, catalytic sites, and nucleation channels to manage Iron/oxygen chemistry: a review for: current opinion in chemical biology/bioinorganic chemistry: Iron biochemistry. Curr Opin Chem Biol 15(2):304–311
28. Yang DC, Jiang X, Elliott RL, Head JF (2002) Antisense ferritin oligonucleotides inhibit growth and induce apoptosis in human breast carcinoma cells. Anticancer Res 22(3):1513–1524
29. Lobello N, Biamonte F, Pisanu ME, Faniello MC, Jakopin Ž, Chiarella E, Giovannone ED, Mancini R, Ciliberto G, Cuda G (2016) Ferritin heavy chain is a negative regulator of ovarian cancer stem cell expansion and epithelial to mesenchymal transition. Oncotarget 7(38):62019–62033
30. Min PJRC (2015) Role of ferritin in Cancer biology. J Cancer Sci Ther 07(5)
31. Li RS, Luo C, Mines M, Zhang JW, Fan GH (2006) Chemokine CXCL12 induces binding of ferritin heavy chain to the chemokine receptor CXCR4, alters CXCR4 signaling, and induces phosphorylation and nuclear translocation of ferritin heavy chain. J Biol Chem 281(49):37616–37627. https://doi.org/10.1074/jbc.M607266200
32. Coffman LG, Parsonage D, D'Agostino R, Torti FM, Torti SV (2009) Regulatory effects of ferritin on angiogenesis. Proc Natl Acad Sci U S A 106(2):570–575. https://doi.org/10.1073/pnas.0812010106
33. Cozzi A, Levi S, Corsi B, Santambrogio P, Campanella A, Gerardi G, Arosio P (2003) Role of iron and ferritin in TNFalpha-induced apoptosis in HeLa cells. FEBS Lett 537(1–3):187–192
34. Aung W, Hasegawa S, Furukawa T, Saga T (2007) Potential role of ferritin heavy chain in oxidative stress and apoptosis in human mesothelial and mesothelioma cells: implications for asbestos-induced oncogenesis. Carcinogenesis 28(9):2047–2052. https://doi.org/10.1093/carcin/bgm090
35. Coffman LG, Parsonage D, D'Agostino R Jr, Torti FM, Torti SV (2009) Regulatory effects of ferritin on angiogenesis. Proc Natl Acad Sci U S A 106(2):570–575. https://doi.org/10.1073/pnas.0812010106
36. Tesfay L, Huhn AJ, Hatcher H, Torti FM, Torti SV (2012) Ferritin blocks inhibitory effects of two-chain high molecular weight kininogen (HKa) on adhesion and survival signaling in endothelial cells. PLoS One 7(7):e40030. https://doi.org/10.1371/journal.pone.0040030
37. Surguladze N, Thompson KM, Beard JL, Connor JR, Fried MG (2004) Interactions and reactions of ferritin with DNA. J Biol Chem 279(15):14694–14702. https://doi.org/10.1074/jbc.M313348200
38. Thompson KJ, Fried MG, Ye Z, Boyer P, Connor JR (2002) Regulation, mechanisms and proposed function of ferritin translocation to cell nuclei. J Cell Sci 115(Pt 10):2165–2177
39. Ghosh S, Hevi S, Chuck SL (2004) Regulated secretion of glycosylated human ferritin from hepatocytes. Blood 103(6):2369–2376. https://doi.org/10.1182/blood-2003-09-3050
40. Ferring-Apel D, Hentze MW, Galy B (2009) Cell-autonomous and systemic context-dependent functions of iron regulatory protein 2 in mammalian iron metabolism. Blood 113(3):679–687. https://doi.org/10.1182/blood-2008-05-155093